Volume 138 (8) April 2025

Journal of Cell Science

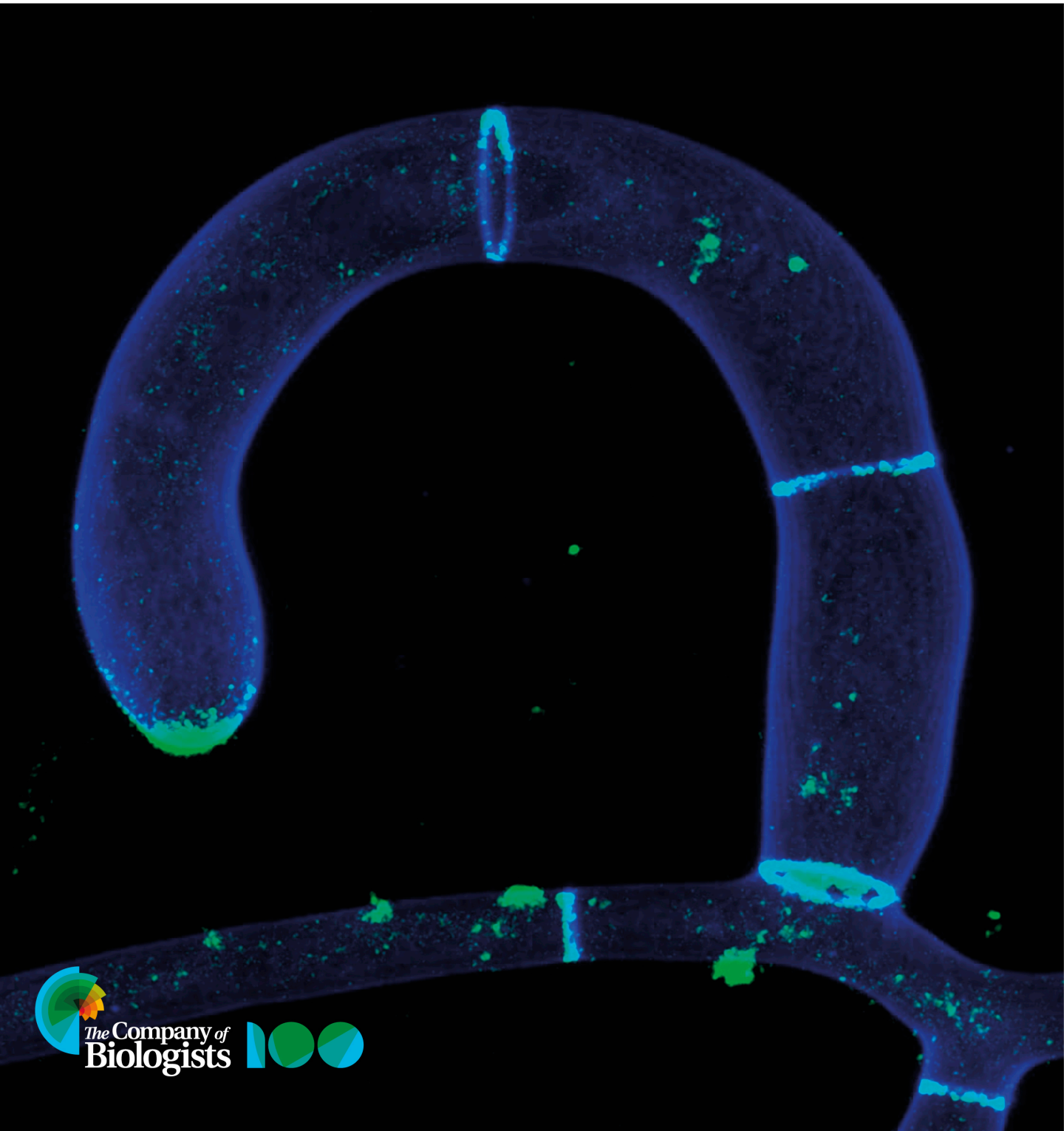

The Company of Biologists

© 2025. Published by The Company of Biologists | Journal of Cell Science (2025) 138, jcs263744. doi:10.1242/jcs.263744

RESEARCH ARTICLE

Cell-end marker proteins are required for hyphal ring formation and size determination of traps in *Arthrobotrys flagrans*

Marius Kriegler[1,*], Valentin Wernet[1,*], Birgit Hetzer[2], Satur Herrero[1], Anlun Wei[1], Jan Wäckerle[1], Imane Dewein[1] and Reinhard Fischer[1,‡]

ABSTRACT

Filamentous fungi grow by apical extension where secretory vesicles are transported long distances by microtubules and by actin prior to fusion with the cell membrane. Apical, membrane-bound cell-end marker proteins (CEMPs) organise the cytoskeletons and thereby the growth machinery. CEMPs have been characterised mainly in *Schizosaccharomyces pombe* and *Aspergillus nidulans*. Here, we studied the role of CEMPs in the nematode-trapping fungus *Arthrobotrys flagrans*. This predatory fungus forms ring-shaped adhesive traps to capture nematodes, such as *Caenorhabditis elegans*. Traps are morphologically and physiologically different from vegetative hyphae and are generated by hyphal turning and fusion of the trap tip cell with the basal hypha. The absence of the membrane-anchored CEMP receptor protein, TeaR, caused a reduction in ring size, whereas deletion of *teaA* or *teaC* largely prevented the formation of ring-shaped hyphae, and most traps appeared as adhesive sticks. Hence, compared to *Schizosaccharomyces pombe* and *Aspergillus nidulans*, loss of function of the CEMPs results in a severe morphological phenotype. The mutant strains also show changes in cell-to-cell communication and hyphal fusion, suggesting novel functions and interconnections with other signalling processes in the cell.

KEY WORDS: Cell end markers, *Arthrobotrys flagrans*, Microtubules, Actin, Nematode-trapping fungi

INTRODUCTION

Polarity establishment and maintenance is crucial for eukaryotic development and especially obvious in filamentous fungi, which grow indefinitely at their tips (Riquelme et al., 2018). Fungal tip elongation depends on continuous delivery of vesicles to the apical dome of the hypha, where they first accumulate in a so-called vesicle supply centre or Spitzenkörper (Grove and Bracker, 1970). From there they are further transported towards the cell membrane for fusion (Riquelme et al., 2018). Vesicle transport and secretion depend on an interplay of microtubules and the actin cytoskeleton. This interplay has been well characterised in *Schizosaccharomyces pombe* and *Aspergillus nidulans* (Takeshita et al., 2013, 2014; Mata and Nurse, 1997; Snaith et al., 2005; Kriegler et al., 2025). In a mutant screening for strains affected in polarity, the first so-called cell-end marker protein (CEMP), tip elongation aberrant 1 (Tea1), was discovered (Snell and Nurse, 1994; Verde et al., 1995). Previous biochemical experiments had already shown that Tea1 can form a large protein complex at the apical membrane, and indeed, different proteins of the complex had been described over time (Mata and Nurse, 1997). The CEMPs Tea1 (TeaA in *A. nidulans*) and Tea4 (TeaC) are delivered to the apex by hijacking the plus-ends of microtubules (Arellano et al., 2002; Mata and Nurse, 1997; Takeshita et al., 2008, 2013; Higashitsuji et al., 2009). The prenylated Mod5 (TeaR) protein reaches the tip, probably through attachment to vesicles, which are transported along microtubules (Snaith and Sawin, 2003; Takeshita et al., 2008). Mod5 is the receptor for other CEMPs which, after recruitment, anchor the actin-forming formin For3 (SepA) to the apex (Taheri-Talesh et al., 2008). Hence, at places where a CEMP complex assembles, actin filaments are polymerising actin cables towards the cytoplasm. In *A. nidulans*, the actin cables guide approaching microtubule plus-ends towards the CEMP complex thereby delivering more of those proteins and promoting more actin cable formation (Manck et al., 2015). This positive feedback mechanism guarantees fast assembly of growth sites. At the same time, actin cables are the tracks for secretory vesicles required for membrane extension and cell wall biosynthesis (Motegi et al., 2001; Schuster et al., 2016), and the fusion of vesicles is deleterious for cell-end marker assemblies, which are subsequently spread out in the membrane. Hence, the accumulation of CEMPs is a self-limiting process, and membrane extension and cell wall biosynthesis occur in a space- and time-restricted manner (Ishitsuka et al., 2015; Takeshita et al., 2014, 2017).

It is largely unknown how the polar-growth machinery can be modulated to form structures different from straight-growing hyphae. An extreme example of a fungal structure where polar growth needs to be modulated are the ring-shaped traps formed by nematode-trapping fungi (NTF). NTF are a diverse group of filamentous fungi able to switch from a saprotrophic to a predatory lifestyle (Jiang et al., 2017). *Arthrobotrys flagrans* is an ascomycete and forms adhesive trapping networks (Youssar et al., 2019). The onset of trap formation depends on the nutritional status and interkingdom signalling between nematodes and the fungus, because traps are only formed under starvation conditions and if nematodes are present (Fischer and Requena, 2022). *A. flagrans* produces several polyketide terpene hybrid molecules, the arthrosporols, which inhibit trap formation under normal growth conditions (Hsueh et al., 2017; Yu et al., 2021). However, if nematodes are present and nutrients are depleted, arthrosporol biosynthesis is inhibited, arthrosporol concentrations decrease and trap formation

[1]Institute for Applied Biosciences, Department of Microbiology, Karlsruhe Institute of Technology (KIT) - South Campus, Fritz-Haber-Weg 4, 76131 Karlsruhe, Germany. [2]Max-Rubner-Institut (MRI) - Federal Research Institute of Nutrition and Food, Haid-und-Neu-Strasse 9, 76131 Karlsruhe, Germany.
*These authors contributed equally to this work

‡Author for correspondence (reinhard.fischer@kit.edu)

R.F., 0000-0002-6704-2569

Handling Editor: Renata Basto
Received 21 November 2024; Accepted 21 March 2025

Journal of Cell Science

Journal of Cell Science (2025) 138, jcs263744. doi:10.1242/jcs.263744

is initiated. *A. flagrans* recognises nematodes through nematode-derived pheromones, the ascarosides (Hsueh et al., 2017; Yu et al., 2021). The fungal receptor for ascaroside sensing has been discovered recently in *A. flagrans* and in *Arthrobotrys oligospora* (Kuo et al., 2024; Hu et al., 2024).

Trap formation starts with the formation of a branch. As a difference to normal branches, trap-forming branches grow in a curved manner to form a ring-like structure that morphologically resembles the clamp connection in basidiomycetes. Besides this morphological differentiation, trap cells are also physiologically different and express trap-specific genes to produce virulence factors (Wernet et al., 2021; Emser et al., 2024). One intriguing aspect is ring closure by hyphal fusion, which requires cell-to-cell communication prior to the fusion event. During cell-to-cell communication, membrane-associated proteins are recruited in an oscillatory manner to the membranes of two approaching hyphae (Haj Hammadeh et al., 2022; Youssar et al., 2019; Wernet et al., 2023). Another very interesting aspect is how curved growth leads to rings with defined diameters. This phenomenon and the underlying cell biological processes are currently not understood, but the obvious changes in polarity suggest that CEMPs play important roles.

Here, we studied the role of CEMPs in *A. flagrans* and show that they are crucial for hyphal curvature, and that TeaR determines the size of the traps.

RESULTS

TeaA, TeaC and TeaR form a dynamic protein complex at the membrane of hyphal tips and at septa

CEMPs have been characterised in *S. pombe*, *A. nidulans* and in the rice blast fungus *Magnaporthe grisea* and the smut fungus *Ustilago maydis* (Rogers et al., 2024; Qu et al., 2022; Valinluck et al., 2014; Kriegler et al., 2025). Orthologues, besides Mod5, also exist in *S. cerevisiae* (Smith and Rose, 2016). CEMPs localise at the tips of growing hyphae, where they form a complex that recruits the formin SepA (in *A. nidulans*), promoting the assembly of actin filaments (Higashitsuji et al., 2009) (Fig. 1A). The actin filaments then direct the deposition of new cell wall material to the complex, thus defining the point of hyphal growth. Here, we identified orthologous proteins in the nematode-trapping fungus *A. flagrans*. They were named TeaA, TeaC and TeaR according to the nomenclature in *A. nidulans*. TeaA consists of 1506 amino acids with multiple kelch-domain repeats in the N-terminal region along with six coiled-coil regions in the C-terminal region. TeaC is a smaller protein, composed of 718 amino acids, with a characteristic SH3 domain. TeaR, with 549 amino acids, harbours CTIM as the final four amino acids of the protein, which is an unusual CAAX-like prenylation motif (Fig. 1B). Overall sequence conservation was low. Structure predictions using AlphaFold provided only very low confidence for all Tea proteins (TeaA pTM=0.36, TeaC pTM=0.21, TeaR pTM=0.19). Most of the sequence was just predicted as disordered regions. Even when

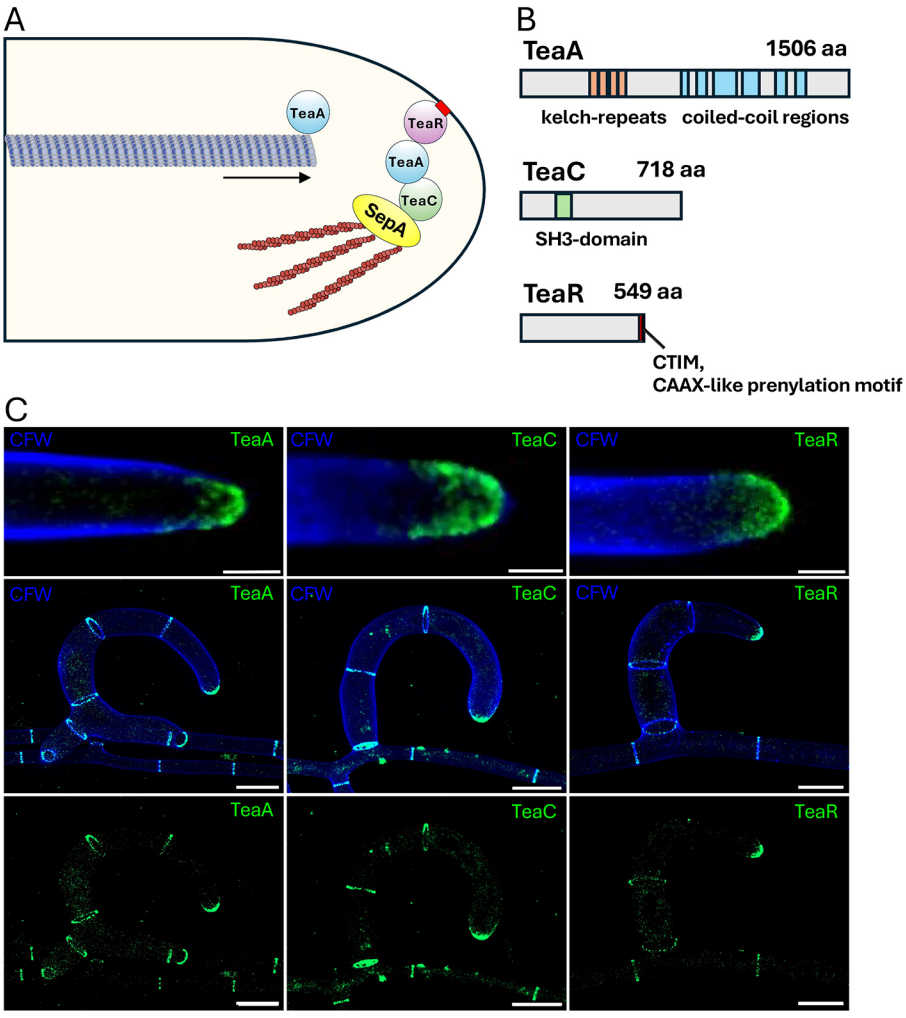

Fig. 1. Analysis of cell end marker proteins in *A. flagrans*. (A) Schematic representation of CEMP localisation and function at the hyphal tip of *A. flagrans*. The proteins TeaA, TeaC and TeaR form a complex that recruits the formin SepA. This complex promotes the assembly of the actin cytoskeleton, directing cell wall deposition and determining the site of hyphal growth. (B) Domain architecture of *A. flagrans* TeaA, TeaC, and TeaR. TeaA (1506 amino acids) contains multiple N-terminal kelch-repeat domains and C-terminal coiled-coil regions. TeaC (718 amino acids) includes an SH3 domain, whereas TeaR (549 amino acids) has a CAAX-like prenylation motif at the C-terminus. (C) Localisation of Tea proteins in hyphal cells. Fluorescence microscopy images show the TeaA, TeaC and TeaR proteins (green) localised at the hyphal tips and septae, stained with calcofluor-white (CFW, blue). Images representative of all hyphae from three independent experimental repeats. Scale bars: traps 10 µm, hyphae 2 µm.

Journal of Cell Science (2025) 138, jcs263744. doi:10.1242/jcs.263744

modelled in a complex, the confidence was very low. Therefore, no further insights into the functioning of the proteins could be inferred from bioinformatic analyses.

To investigate the localisation of the three proteins, we tagged TeaA, TeaC, and TeaR at their respective loci with GFP using a knock-in strategy with homologous recombination, ensuring wild-type expression levels. For TeaA and TeaC, GFP was fused to the C-terminus, whereas TeaR was tagged N-terminally. All three strains exhibited wild type-like phenotypes, indicating full functionality of the tagged proteins. The cell-end markers were always visible at the tips of growing vegetative hyphae and tip cells of traps and at septa (Figs 1C, 2A; Movie 1). We also localised TeaA–GFP in a *teaR*-deletion strain but did not observe differences compared to wild type (WT) (Fig. 2B). This contrasts with findings in *A. nidulans*, where TeaA localisation depended on TeaR (Takeshita et al., 2008). Additionally, we colocalised chitin synthase B (ChsB) with TeaA. The signals at the hyphal tip often overlapped, indicating the site of growth (Fig. 2C). However, TeaA–GFP frequently appeared in extra spots, which did not colocalise with chitin synthase B. These spots probably are the plus-ends of microtubules, where TeaA accumulates. The distribution at the hyphal apical membrane was not uniform, but proteins appeared in a spot-like pattern, suggesting the presence of CEMP clusters. Similarly, in *S. pombe*, it has been demonstrated that CEMPs form dynamic clusters through oligomerisation (Dodgson et al., 2013). Time-resolved observations revealed a highly dynamic localisation pattern of these clusters (Fig. 3A,B; Movie 2). The clusters persisted for between 30 and 180 s before disassembling and reappearing. Their number and distribution changed over time, often resulting in a more crescent-like appearance at the hyphal tip. However, the apical dome did not show pronounced membrane extensions at the places of the cell-end marker complexes at our resolution of the cell shape as was observed previously in *A. nidulans* (Ishitsuka et al., 2015) (Fig. 3C). Therefore, we assumed that the correlation of growth with the position of the cell-end marker complexes would be more obvious when changes of the growth direction are necessary. To test this hypothesis, we tracked TeaA localisation during hyphal fusion. During fusion events, hyphae engage in cellular communication. This signalling results in the reorientation of a growing hypha towards its fusion partner, accompanied by a repositioning of the polar growth site. When we localised TeaA during this event, the protein clearly moved to the new site of growth (Fig. 3D; Movie 3), suggesting that cell-end marker relocation is a prerequisite for growth orientation.

TeaA, TeaC and TeaR play overlapping and distinct roles in hyphal growth and trap formation

To elucidate the functions and potential roles of CEMPs in trap formation, we deleted all three *tea* genes and generated corresponding re-complemented strains. Additionally, an overexpression strain of *teaA* was constructed under the control of the *A. nidulans* constitutive *oliC* promoter (ATPase subunit 9) (Ward and Turner, 1986). Deletion and overexpression of *teaA* caused the most severe growth defect with fewer aerial hyphae at the colony periphery and increased aerial hyphae at the centre (Fig. 4A,C). The Δ*teaC* strain also exhibited growth defects and reduced aerial hyphae, albeit to a lesser extent, while the Δ*teaR* strain showed only a slight reduction in growth.

To further compare the phenotypes of the strains, we inoculated WT and *tea* mutant strains of *A. flagrans* and *A. nidulans* on minimal medium. The Δ*teaA*, Δ*teaC* and particularly the *teaA* overexpression strains showed a tendency for hyperbranching, but no curved hyphae (Fig. 5) in contrast to what has been described in *A. nidulans* (Takeshita et al., 2008). Only the Δ*teaR* strain exhibited meandering growth, without hyperbranching. This pattern was comparable to the pattern in *A. nidulans*, where *teaA* deletion induced hyperbranching (Takeshita et al., 2008), but neither the Δ*teaA* nor Δ*teaC* strains displayed curved growth under our growth conditions. These results suggest that TeaR serves a distinct role compared to TeaA and TeaC, whose absence caused similar phenotypes.

The Δ*teaA*, Δ*teaC* and the *teaA* overexpression strains failed to close the rings of the traps (Fig. 6A). 100% of the traps of the Δ*teaA* and the *teaA* overexpression strains, and ∼80% of the traps of the Δ*teaC* strains, had a stick-like appearance. Despite these abnormalities, the sticky traps remained fully functional and were capable of capturing and digesting nematodes (Fig. 6B). In the Δ*teaR* strain, hyphae were still able to fuse and formed ring-like traps. The Δ*teaR* strain produced also trap numbers similar to WT,

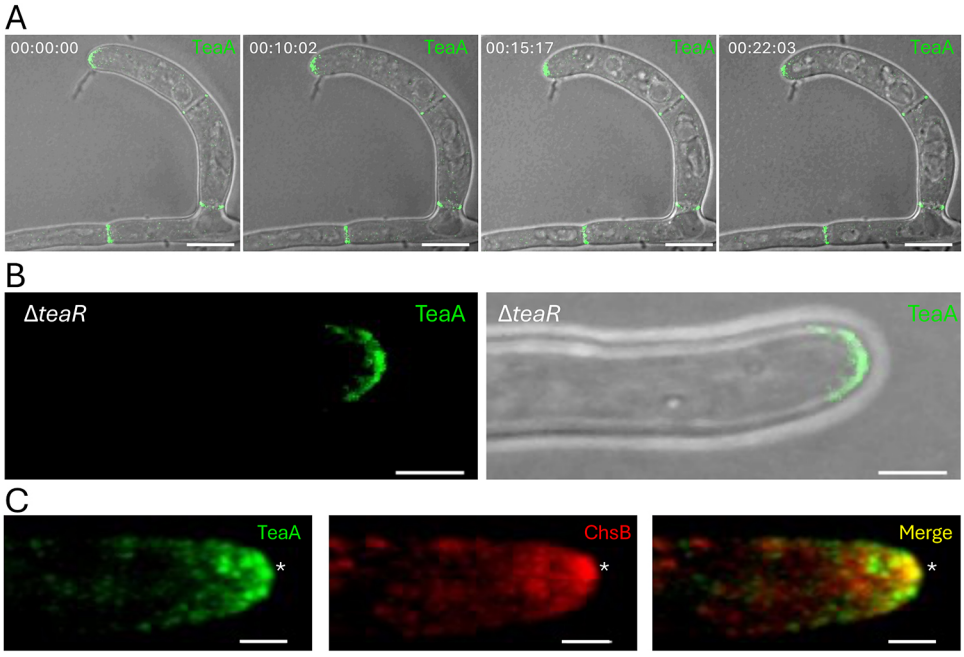

Fig. 2. Analysis of TeaA localisation in traps and the *teaR*-deletion strain, and colocalisation with chitin synthase B. (A) Fluorescence microscopy images taken from Movie 1 showing TeaA–GFP in traps. Time is in hh:mm:ss. (B) TeaA localisation in the *teaR*-deletion strain. (C) Colocalisation of TeaA–GFP and chitin synthase B (ChsB). The asterisks mark the overlapping spot and the probable areas of growth. Images representative of three repeats. Scale bars: traps 10 µm, hyphae 2 µm.

Journal of Cell Science (2025) 138, jcs263744. doi:10.1242/jcs.263744

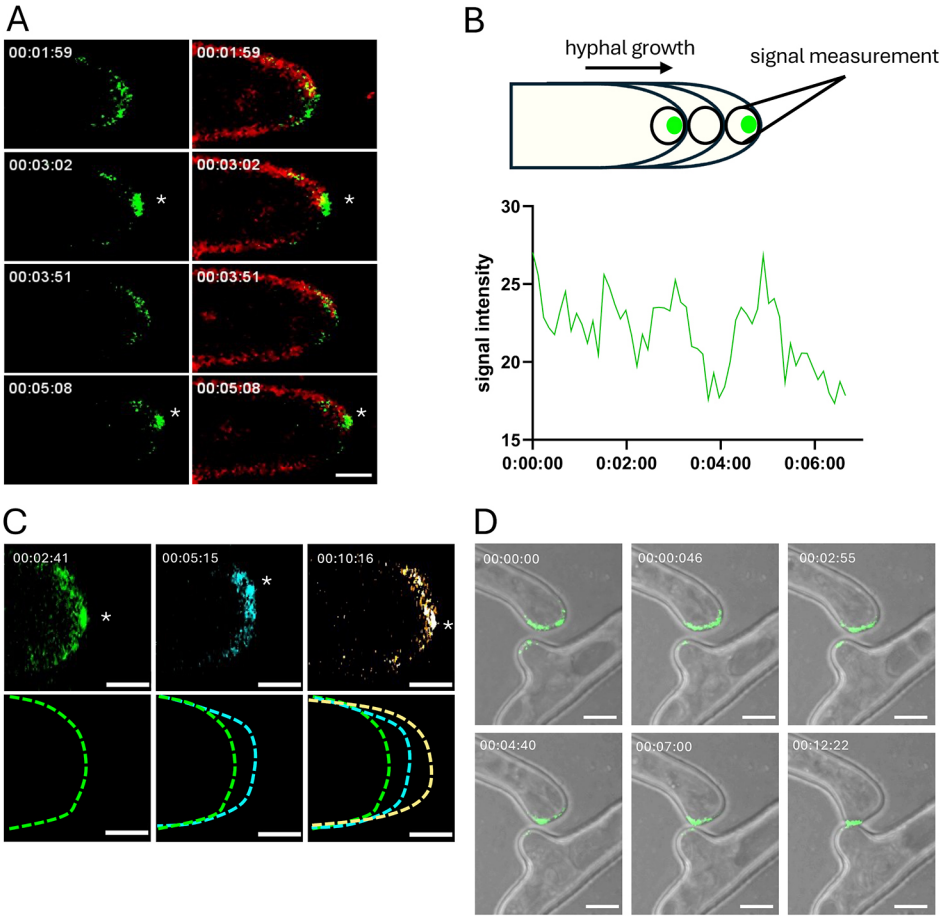

Fig. 3. Tea protein localisation and dynamics. (A) Fluorescence microscopy images taken from Movie 2 showing TeaA–GFP at a hyphal tip. The cell shape was visualised by FM4-64 membrane staining. (B) Signal intensity quantification along hyphal growth from Movie 2. The intensity was measured as seen in the scheme above. (C) Green, cyan and yellow channels correspond to different localisations of TeaA accumulations at the indicated time points. The dashed lines indicate the cell shape. (D) Snapshots taken from a time-lapse movie of TeaA protein dynamics at hyphal tips during hyphal fusion. The asterisks mark the position of the TeaA clusters and the probable areas of growth. Images representative of all hyphae from three independent experimental repeats. Times are hh:mm:ss. Scale bars: 2 µm.

whereas the other mutant strains produced very few traps (Fig. 6C). The mutant phenotype was fully restored in re-complemented strains. To confirm the identity of the stick-like structures as traps, we used the effector protein NipA fused to RFP. NipA is specifically expressed in traps and localises in vesicles at the inner rim of the traps (Emser et al., 2024) (Fig. 6A). In the stick-like traps, NipA was expressed, proving the differentiation of the hyphae into traps. However, as a difference to WT, NipA did not concentrate at one side of the hypha, raising the question of whether the Tea proteins or the curvature of traps is required for internal vesicle sorting.

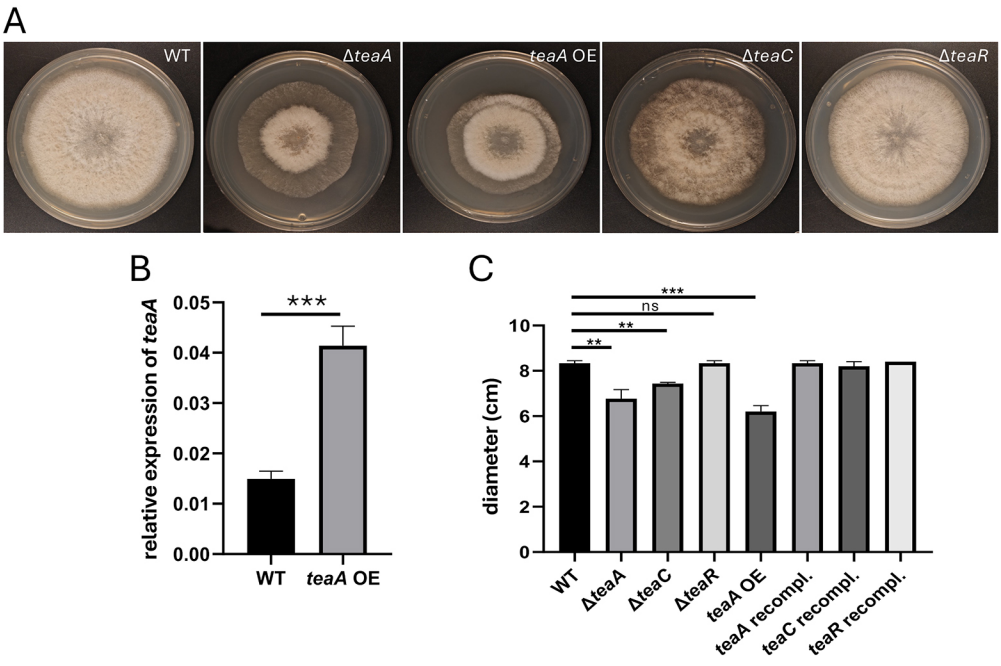

Fig. 4. Phenotype of *tea* mutant strains of *A. flagrans*. (A) Colony morphology of WT, Δ*teaA*, *teaA* overexpression (*teaA* OE), Δ*teaC* and Δ*teaR* mutants of *A. flagrans* on PDA after 5 days of growth. (B) Expression levels of *teaA* were quantified by qRT-PCR in WT and the *tea*-overexpression strain. (C) Growth assay of WT and the tea mutants. The diameter of each strain was measured after 6 days. Results in B and C are mean±s.d. (n=3). $^{**}P$<0.01; $^{***}P$<0.001; ns, not signifciant (two-tailed unpaired t-test).

Journal of Cell Science (2025) 138, jcs263744. doi:10.1242/jcs.263744

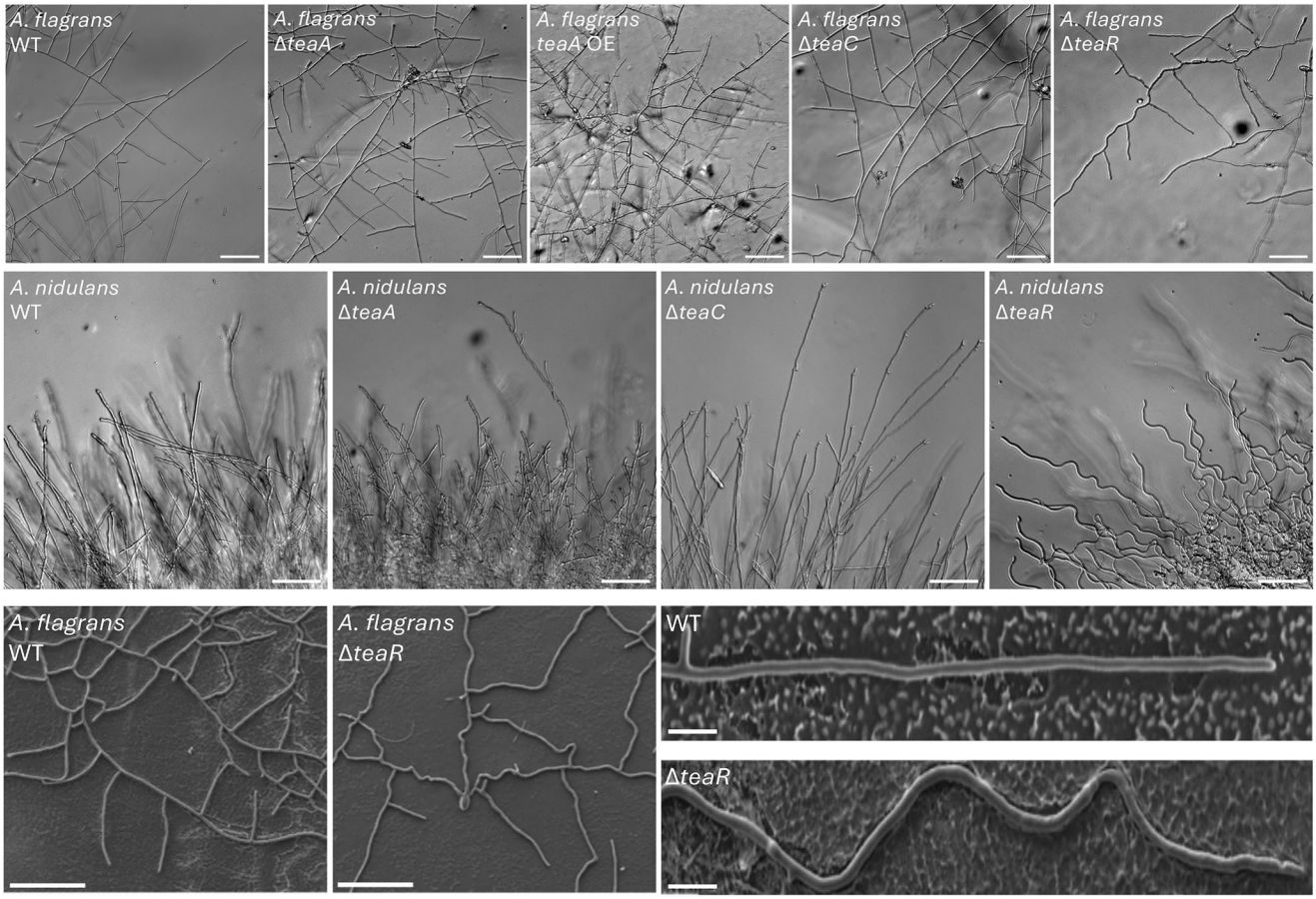

Fig. 5. Hyphal growth of *tea* mutants of *A. flagrans* and *A. nidulans*. (A) Hyphal growth of *A. flagrans* and *A. nidulans* WT, Δ*teaA*, *teaA* overexpression (*teaA* OE), Δ*teaC* and Δ*teaR* on MM medium. Only the Δ*teaR* strain exhibited curved growth. The re-complemented strains restored WT phenotypes. Images below were obtained by cryo-SEM. Images representative of all hyphae from three independent experimental repeats. Scale bars: 100 µm, cryo-SEM single hyphae 10 µm.

In the Δ*teaR* strain, traps retained the ability to bend and fuse but were significantly smaller in diameter (Fig. 6D). Whereas WT traps measured between 449 µm (±191, s.d) in diameter, the traps of the Δ*teaR* strain were only 256 µm (±119) (n=60).

TeaA and TeaC, but not TeaR, are required for hyphal fusion

Observing hyphal growth revealed that the *teaA* overexpression, *teaA*- and *teaC*-deletion strains exhibited distinct colony morphologies compared to WT. *A. flagrans* typically undergoes extensive hyphal fusion, unlike fungi such as *A. nidulans*, resulting in a structured and organised network of fused hyphae across the colony (Haj Hammadeh et al., 2022). However, the *teaA* overexpression and the *teaA*- and *teaC*-deletion strains displayed a more disorganised hyphal network, primarily due to the absence of hyphal fusions (Fig. 7A).

To investigate this further, the WT and *tea*-deletion strains were inoculated on low-nutrient medium, and images were captured from different locations within the colony. Then the number of hyphal fusion events was quantified. This experiment demonstrated a significant reduction in hyphal fusion events in the *teaA* overexpression and the *teaA*- and *teaC*-deletion strains (Fig. 7B). The Δ*teaR* strain did not show any signs of abnormal hyphal fusion. Normal hyphal fusion is typically characterised by the bending and subsequent fusion of a hyphal tip with a nearby hypha. Although normal fusion was rarely observed in the Δ*teaA*, *teaA* OE and Δ*teaC* strains, their hyphae frequently grew along each other (Fig. 7A). Occasionally, single fusion events occurred between these closely growing hyphae, indicating that fusion is still possible but that the recognition and reorientation towards a fusion partner were impaired in these mutant strains.

DISCUSSION

The principles of hyphal tip extension are conserved across filamentous fungi, relying on the continuous delivery of vesicles and the spatial organisation of both the microtubule and the actin cytoskeleton. These cytoskeletal networks are interdependent, in part due to the CEMP complexes located at the hyphal tips. Microtubules direct the assembly of actin cables, whereas actin filaments capture microtubule plus-ends and guide them toward these complexes (Fig. 8) (Manck et al., 2015; Kriegler et al., 2025). The system is self-regulating – an increase in CEMPs leads to an increase in vesicle fusion events and subsequent dilution of the protein complexes at the tip. Phenotypes of deletion mutants are not very strong, although the original mutagenesis approach for temperature-sensitive mutants in *S. pombe* accounted for putative lethality (Verde et al., 1995). However, the first gene identified, *tea1*, turned out not to be essential, but its mutation produced a rather mild phenotype with bent or T-shaped cells (Mata and Nurse, 1997). Likewise, deletion of the *tea1* orthologue in *A. nidulans*, *teaA*, produced zig-zag-growing hyphae when grown on agar-coated microscope slides (Takeshita et al., 2008). Meandering hyphae have also been observed in *Neurospora crassa*, for example, upon treatment with benomyl to disrupt microtubules or upon deletion of the heavy chain of cytoplasmic dynein, resulting in the

Journal of Cell Science (2025) 138, jcs263744. doi:10.1242/jcs.263744

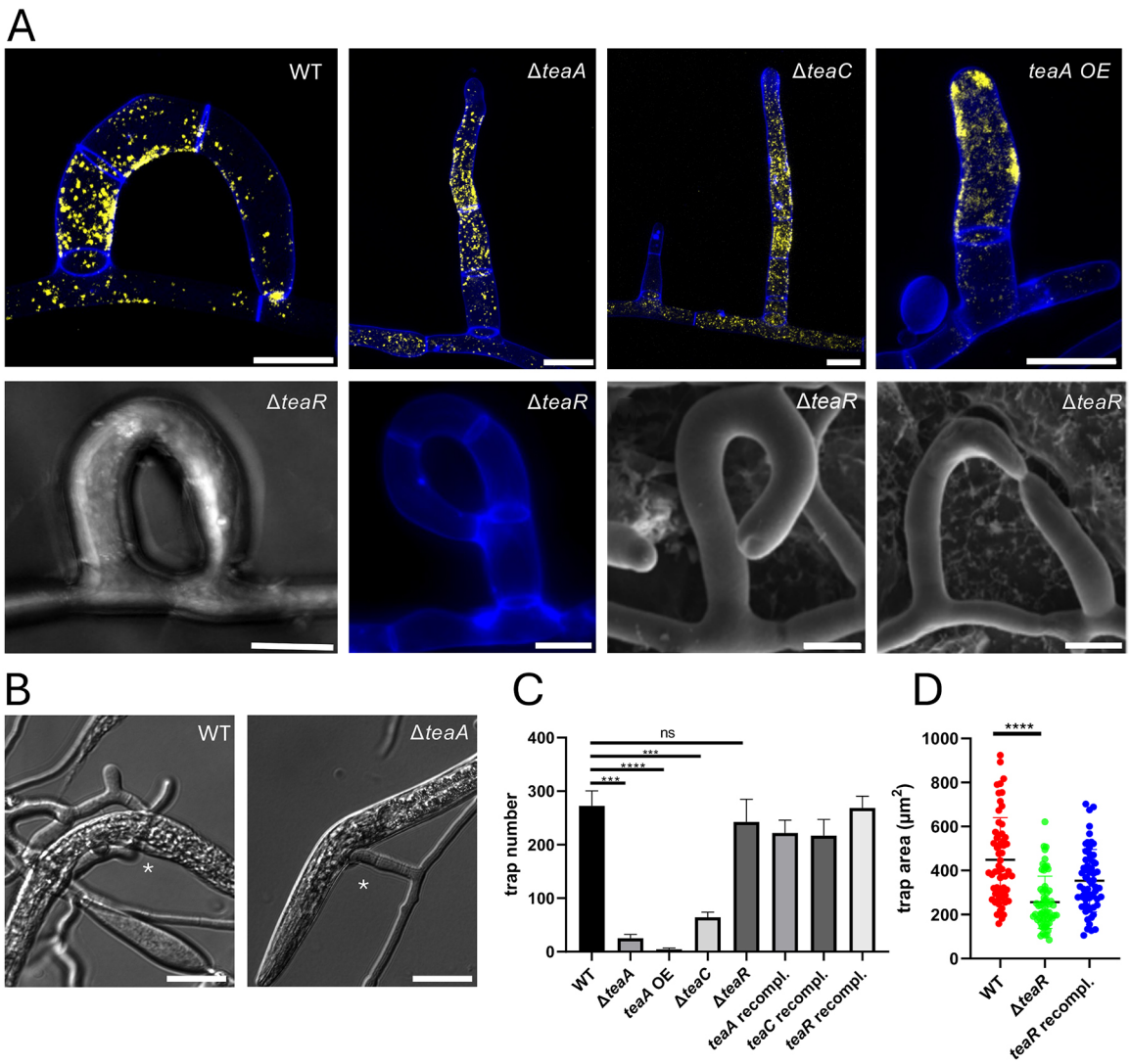

Fig. 6. Analysis of trap formation of *tea* mutant strains. (A) Trap formation in WT, Δ*teaA*, *teaA* overexpression (*teaA* OE), Δ*teaC* and Δ*teaR* mutant strains on LNM after incubation with nematodes. Cell wall is stained with Calcofluor White (blue), and the NipA protein (yellow) confirms the trap character. The Δ*teaA*, Δ*teaC* and *teaA* OE strains are no longer capable of forming closed traps whereas the Δ*teaR* strain can still curve and fuse to form traps. These traps are significantly smaller compared to WT. The last two pictures in the row were obtained with Cryo-SEM. Scale bars: 10 µm. (B) Captured nematode (asterisk) by WT and Δ*teaA*. Scale bars: 20 µm. (C) WT and *tea* mutant strains were inoculated on LNM with nematodes for 24 h. Traps were counted in an area of about 0.5 cm^2 (n=3). Trap formation in *tea* mutant strains is significantly impaired in Δ*teaA*, Δ*teaC* and *teaA* OE strains. In contrast, trap numbers in the Δ*teaR* and re-complementation strains are comparable to WT. (D) Measurement of the trap area in WT and Δ*teaR* strains shows a significant reduction in trap size in the Δ*teaR* strain (n=60 for each strain). Results in C and D are mean±s.d. ***P<0.001; ****P<0.0001; ns, not signifciant (two-tailed unpaired t-test).

so-called ‘ropy’ mutants (Riquelme et al., 1998, 2002). The ropy phenotype has been attributed to microtubule perturbation, which disrupts organelle dynamics and positioning. It has been proposed that the positioning of the Spitzenkörper, the cytoskeleton and the growth direction of hyphae are tightly correlated.

In this study, we demonstrate that both TeaA and TeaC are essential for directional growth during trap formation in *A. flagrans*. However, the mechanisms underlying the preferential positioning of cell-end markers on one side of the hyphal apex remain unclear and might involve specific membrane domains (Takeshita et al., 2008, 2012). Our findings further reveal that TeaA and TeaC contribute to trap formation and to hyphal fusion, potentially through an unidentified link between CEMPs and signalling pathways. In *S. pombe*, cell-end markers and GTPases, such as Cdc42, are crucial for establishing cell polarity (Verde et al., 1995; Miller and Johnson, 1994). This is evident in the new end take-off (NETO) phase, where, following cell division, polarity markers promote the activation of a new polarity site, enabling the cell to switch from monopolar to bipolar growth (Mitchison and Nurse, 1985). Previous research in *S. pombe* has highlighted the role of cell-end markers in regulating the recruitment of guanine-exchange factors (GEFs), including Scd1 and Gef1, to the cell ends (Tatebe et al., 2008; Kokkoris et al., 2014; Tay et al., 2018). Furthermore, GTPase-activating proteins (GAPs) such as Rga4, which negatively regulate Cdc42, are actively excluded from cell tips by Tea proteins to maintain stable polarity. Cdc42 participates in multiple signalling pathways, including stress MAPK pathways (Tatebe et al., 2005; Perez et al., 2020). It is possible that pathways essential for trap induction and hyphal fusion are affected in cell-end marker mutants. In *Saccharomyces cerevisiae*, the KEL1 protein, an orthologue of

Journal of Cell Science (2025) 138, jcs263744. doi:10.1242/jcs.263744

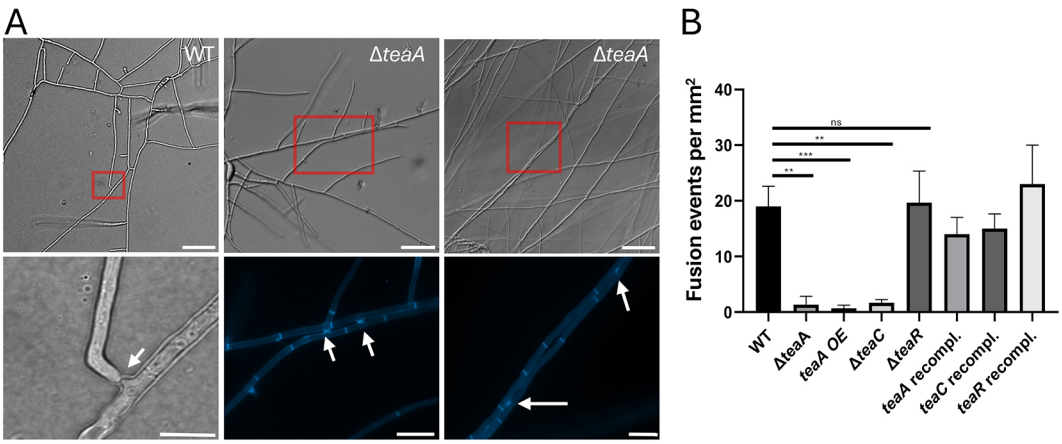

Fig. 7. Analysis of hyphal fusion in *tea* mutant strains. (A) In WT, hyphal fusion is characterised by the reorientation of the hyphal tip, leading to fusion at the tip end. In contrast, most fusion events in Δ*teaA* mutant strains exhibit parallel growth of two hyphae with only a small connecting tube between them. The red panels refer to fusion events. A magnified view of the red panel is shown below each picture. The arrows indicate where hyphal fusion occurs. Hyphae in cyan are stained with Calcofluor White. (B) WT, Δ*teaA*, *teaA* overexpression (*teaA* OE), Δ*teaC* and Δ*teaR* mutant strains and re-complementation strains were inoculated on LNM, and images were captured using 10× objective magnification across various regions (n=3). The number of hyphal fusion events was quantified, excluding those involving parallel-growing hyphae. Deletion strains of *teaA* and *teaC*, as well as the overexpression of *tea*, showed mostly abnormal hyphal fusion events, whereas the *teaR*-deletion strain and re-complementation strains look like WT. Results are mean±s.d. **P<0.01; ***P<0.001; ns, not signifciant (two-tailed unpaired t-test). Scale bars: 50 µm, magnification 10 µm.

TeaA, has also been shown to play a role in cell fusion and mating (Philips and Herskowitz, 1998; Smith and Rose, 2016). The hyphal fusion defects observed in this study might also result from an inability to properly regulate hyphal reorientation towards a fusion partner. This hypothesis is supported by the fact that hyphae were still capable of fusing over very short distances.

Interestingly, deletion of *teaA* and *teaC* impairs polarity, but TeaA overexpression caused defects in cell fusion and trap formation. This suggests that maintaining a fine balance of these proteins is crucial, as disruption of this balance results in polarity dysfunction.

The phenotype of the Δ*teaR* mutant differed from that of the *teaC* and *teaA* mutants, as it was still able to form closed traps, but with a smaller diameter compared to WT. This suggests that TeaR is not essential for anchoring TeaA and TeaC at the membrane but plays a crucial role in their precise positioning. Other studies also describe TeaR as a highly dynamic protein, challenging the conventional understanding of the ligand–receptor system (Snaith et al., 2005; Bicho et al., 2010). The dynamics of Tea cluster formation remain poorly understood, and it is likely that additional factors are involved. In contrast, no significant differences were observed between the WT and the Δ*teaR* strain in trap formation and cell fusion, highlighting a clear functional divergence in TeaA and TeaC compared to TeaR. The fact that the *ΔteaR* strain showed no difference in the TeaA–GFP pattern raises further questions. It is possible that TeaR plays a different role in *A. flagrans* compared to *A. nidulans*, which is also reflected in the imperfect CAAX motif. However, the Δ*teaR* strain exhibited a curved growth pattern, similar to *A. nidulans*, further supporting the notion that TeaR facilitates the precise localisation of TeaA and TeaC but is not required for their fundamental functions.

MATERIALS AND METHODS

Strains and culture conditions

A. flagrans was cultivated on potato dextrose agar (PDA; 2.4% potato dextrose broth and 1.5% agar, Carl Roth) at 28°C. *A. nidulans* strains were cultivated on minimal medium (MM) at 37°C (Hill and Käfer, 2001). All *A. flagrans* strains derived from CBS349.94 are listed in Table S1. The *A. nidulans* strains are described in Higashitsuji et al. (2009) and Takeshita et al. (2008). Transgenic strains of *A. flagrans* were generated by protoplast transformation (Youssar et al., 2019). The N2 *C. elegans* strain was obtained from Prof. Dr. Ralf Baumeister (University of Freiburg) and cultured following the protocol described in WormBook (doi: 10.1895/wormbook.1.101.1).

Plasmids and strains constructions

For plasmid cloning, competent TOP10 *Escherichia coli* cells were used. All plasmids and primers used in this study are listed in Tables S2 and S3. For the localisation studies, TeaA and TeaC were C-terminally tagged *in locus*, and TeaR was N-terminally tagged *in locus* using a homologous recombination strategy. For the C-terminal tagging, a 1 kb fragment of the C-terminal open reading frame (ORF) and a 1 kb fragment of the terminator region were amplified from genomic DNA of *A. flagrans*. Additionally, a GFP and *hph* cassette were amplified from the plasmid pNH57 and assembled via Gibson assembly into the plasmid pJET 1.2. For GFP tagging of TeaR, a 1 kb fragment of the promoter region and a 1 kb fragment of the N-terminal open reading frame were amplified by PCR from genomic DNA and assembled in the order *teaR(p)::GFP::teaR(1 kb)::hph* into linearised pJET1.2.

Deletion strains were generated via homologous recombination. For this, 1 kb flanks of the 5′ region and a 1 kb fragment of the 3′ region were amplified, and an *hph* cassette was assembled between them via Gibson assembly into pJET1.2. Homologous recombination was confirmed by Southern blot analysis. For each *tea* re-complementation, a vector was constructed in which the respective native *tea* promoter and ORF were amplified from WT genomic DNA and then cloned into the pJet1.2 backbone via Gibson assembly. Additionally, a geneticin resistance cassette was amplified and incorporated into the vector. This construct was then transformed into the respective deletion strain. Geneticin-resistant strains were subsequently selected based on their phenotype to confirm whether the re-complementation was successful.

Microscopy, trap induction and qRT-PCR

For microscopy fungal strains were either inoculated slides with LNM (1 g/l KCl, 0.2 g $MgSO_4{\cdot}7H_2O$, 0.4 mg $MnSO_4{\cdot}4H_2O$, 0.88 mg $ZnSO_4{\cdot}7H_2O$, 3 mg $FeCl_3{\cdot}6H_2O$, 15 g agar, pH 5.5) or MM (Martinelli, 1994). Spores were placed on 2×2 cm agar pads and incubated by 28°C for 12–24 h in darkness. For the induction of traps, ∼1000 *C. elegans* nematodes were added to the LNA agar slides. Trap counting was performed in triplicate, using three separate agar slides, each with a counted area of 1×1 cm in diameter.

For quantifying fusion events and evaluating trap area, fungi were incubated on LNA and images were randomly captured at different positions with a 10× objective lens. Trap area was measured by outlining the inner circle of each trap using ImageJ (Fiji). Fusion events were also quantified in

Journal of Cell Science (2025) 138, jcs263744. doi:10.1242/jcs.263744

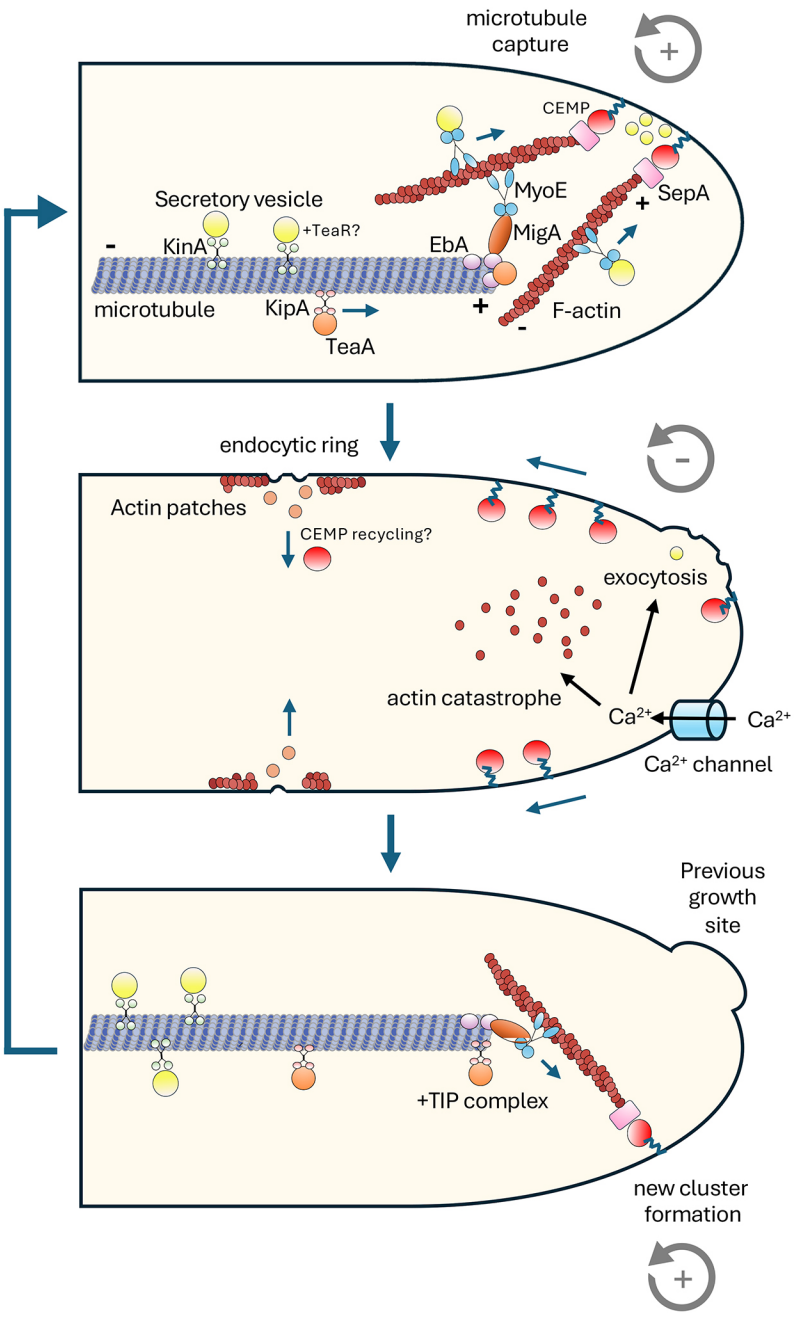

Fig. 8. Model for the mode of action of Tea proteins in filamentous fungi. Tea proteins are transported along microtubules either directly as cargo of the kinesin VII KipA (TeaA) or in the case of the prenylated TeaR receptor at vesicles. KipA and TeaA accumulate at the microtubule plus-end. A small Tea complex at the membrane assembles actin filaments along which microtubule plus-ends are pulled to merge in one point and deliver more Tea proteins. This positive feed-back loop leads to more actin filaments. Secretory vesicles, which are transported along microtubules by conventional kinesin as motor, are then reloaded onto actin filaments. Vesicles containing cell-wall biosynthesis enzymes accumulate around the Tea-complex sites. A link between Tea proteins and Cdc42 has been shown in *S. pombe* but is yet to be proven in filamentous fungi. Middle and lower panels: Pulsed Ca^{2+} influx induces fusion of the secretory vesicles with the membrane and cause actin catastrophe. Cell wall will be synthesised at that place. Membrane integration disturbs the integrity of the Tea complexes, which then dissolve. Some of them will be internalised in the endocytic ring, and others give rise to new actin filament formation.

ImageJ, counting only clearly visible fusion events that did not involve parallel hyphae.

Live-cell imaging of *A. flagrans* was performed using a confocal microscope (Airyscan LSM900, Carl Zeiss) with a 63× NA 1.4 oil objective lens (DIC M27). Time series were acquired with a gallium arsenide phosphide photomultiplier tube (GaAsP-PMT) detector, using 488 or 561 nm excitation. Differential interference contrast (DIC) images were captured on a Zeiss AxioImager Z.1 equipped with an AxioCam MR. High-resolution Cryo-Scanning electron microscopy (cryo-SEM) was performed as described previously, allowing an artefact-free *in situ* examination of the hyphal morphology during trap formation (Braun et al., 2018).

RNA extraction and qRT-PCR was performed as described in Youssar et al. (2019). Primer sequences are given in Table S3.

Statistical analysis

Unless otherwise stated, experiments were performed in triplicate. *P*-values were calculated using a *t*-test in GraphPad Prism 9. Data presented in column graphs or scatter plots represent the mean±standard deviation (s.d.), as indicated in the figure legends.

Acknowledgements

We thank B. Schreckenberger and E. Wohlmann for excellent technical assistance. The work was supported by core funding of the Karlsruhe Institute of Technology (KIT).

Competing interests

The authors declare no competing or financial interests.

Author contributions

Conceptualization: R.F.; Data curation: M.K., V.W.; Formal analysis: V.W.; Funding acquisition: R.F.; Investigation: M.K., V.W., S.H., A.W., J.W., I.D.; Methodology: M.K., V.W., B.H., S.H., A.W., J.W., I.D.; Project administration: R.F., V.W.; Supervision: R.F., V.W.; Validation: V.W.; Visualization: M.K., V.W.; Writing – original draft: M.K.; Writing – review & editing: R.F.

Funding

The work was supported by the Deutsche Forschungsgemeinschaft (DFG) (Fi-459 26/1). V.W. was supported by the Deutsche Bundesstiftung Umwelt (DBU).

Data and resource availability

All strains are available upon request from R.F.

References

Arellano, M., Niccoli, T. and Nurse, P. (2002). Tea3p is a cell end marker activating polarized growth in *Schizosaccharomyces pombe*. *Curr. Biol.* **12**, 751-756. doi:10.1016/S0960-9822(02)00821-7

Bicho, C. C., Kelly, D. A., Snaith, H. A., Goryachev, A. B. and Sawin, K. E. (2010). A catalytic role for Mod5 in the formation of the Tea1 cell polarity landmark. *Curr. Biol.* **20**, 1752-1757. doi:10.1016/j.cub.2010.08.035

Braun, H., Woitsch, L., Hetzer, B., Geisen, R., Zange, B. and Schmidt-Heydt, M. (2018). *Trichoderma harzianum*: inhibition of mycotoxin producing fungi and toxin biosynthesis. *Int. J. Food Microbiol.* **280**, 10-16. doi:10.1016/j.ijfoodmicro.2018.04.021

Dodgson, J., Chessel, A., Yamamoto, M., Vaggi, F., Cox, S., Rosten, E., Albrecht, D., Geymonat, M., Csikasz-Nagy, A., Sato, M. et al. (2013). Spatial segregation of polarity factors into distinct cortical clusters is required for cell polarity control. *Nat. Commun.* **4**, 1834. doi:10.1038/ncomms2813

Emser, J., Wernet, N., Hetzer, B., Wohlmann, E. and Fischer, R. (2024). The small cysteine-rich virulence factor NipA of *Arthrobotrys flagrans* interferes with cuticle integrity of *Caenorhabditis elegans*. *Nat. Commun.* **15**, 5795. doi:10.1038/s41467-024-50096-4

Fischer, R. and Requena, N. (2022). Small-secreted proteins as virulence factors in nematode-trapping fungi. *Trends Microbiol.* **30**, 616-617. doi:10.1016/j.tim.2022.03.005

Grove, S. N. and Bracker, C. E. (1970). Protoplasmic organization of hyphal tips among fungi: vesicles and Spitzenkörper. *J. Bacteriol.* **104**, 989-1009. doi:10.1128/jb.104.2.989-1009.1970

Haj Hammadeh, H., Serrano, A., Wernet, V., Stomberg, N., Hellmeier, D., Weichert, M., Brandt, U., Sieg, B., Kanofsky, K. et al. (2022). A dialogue-like cell communication mechanism is conserved in filamentous ascomycete fungi and mediates interspecies interactions. *Proc. Natl. Acad. Sci. USA* **119**, e2112518119. doi:10.1073/pnas.2112518119

Higashitsuji, Y., Herrero, S., Takeshita, N. and Fischer, R. (2009). The cell end marker protein TeaC is involved in both growth directionality and septation in *Aspergillus nidulans*. *Eukaryot. Cell* **8**, 957-967. doi:10.1128/EC.00251-08

Hill, T. W. and Käfer, E. (2001). Improved protocols for *Aspergillus* minimal medium: trace element and minimal medium salt stock solutions. *Fungal Genet. Newsletter* **48**, 20-21. doi:10.4148/1941-4765.1173

Hsueh, Y. P., Gronquist, M. R., Schwarz, E. M., Nath, R. D., Lee, C. H., Gharib, S., Schroeder, F. C. and Sternberg, P. W. (2017). Nematophagous fungus *Arthrobotrys oligospora* mimics olfactory cues of sex and food to lure its nematode prey. *eLife* **6**, e20023. doi:10.7554/eLife.20023

Hu, X., Hoffmann, D., Wang, M., Schuhmacher, L., Stroe, M. C., Schreckenberger, B., Elstner, M. and Fischer, R. (2024). GprC of the nematode-trapping fungus *Arthrobotrys flagrans* activates mitochondria and reprograms fungal cells for nematode hunting. *Nat. Microbiol.* **9**, 1752-1763. doi:10.1038/s41564-024-01731-9

Ishitsuka, Y., Savage, N., Li, Y., Bergs, A., Grün, N., Kohler, D., Donnelly, R., Nienhaus, G. U., Fischer, R. and Takeshita, N. (2015). Superresolution microscopy reveals a dynamic picture of cell polarity maintenance during directional growth. *Sci. Adv.* **1**, e1500947. doi:10.1126/sciadv.1500947

Jiang, X., Xiang, M. and Liu, X. (2017). Nematode-trapping fungi. *Microbiol. Spectr.* **5**, FUNK-0022. doi:10.1128/microbiolspec.FUNK-0022-2016

Kokkoris, K., Gallo Castro, D. and Martin, S. G. (2014). The Tea4-PP1 landmark promotes local growth by dual Cdc42 GEF recruitment and GAP exclusion. *J. Cell Sci.* **127**, 2005-2016. doi:10.1242/jcs.142174

Kriegler, M., Herrero, S. and Fischer, R. (2025). Where to grow and where to go. *Fungal Genet. Biol.* **178**, 103983. doi:10.1016/j.fgb.2025.103983.

Kuo, C. Y., Tay, R. J., Lin, H. C., Juan, S. C., Vidal-Diez De Ulzurrun, G., Chang, Y. C., Hoki, J., Schroeder, F. C. and Hsueh, Y. P. (2024). The nematode-trapping fungus *Arthrobotrys oligospora* detects prey pheromones via G protein-coupled receptors. *Nat. Microbiol.* **9**, 1738-1751. doi:10.1038/s41564-024-01679-w

Manck, R., Ishitsuka, Y., Herrero, S., Takeshita, N., Nienhaus, G. U. and Fischer, R. (2015). Genetic evidence for a microtubule-capture mechanism during polarised growth of *Aspergillus nidulans*. *J. Cell Sci.* **128**, 3569-3582. doi:10.1242/jcs.169094

Martinelli, S. D. (1994). Media. *Prog. Ind. Microbiol.* **29**, 829-832.

Mata, J. and Nurse, P. (1997). *tea1* and the microtubular cytoskeleton are important for generating global spatial order within the fission yeast cell. *Cell* **89**, 939-949. doi:10.1016/S0092-8674(00)80279-2

Miller, P. J. and Johnson, D. I. (1994). Cdc42p GTPase is involved in controlling polarized cell growth in *Schizosaccharomyces pombe*. *Mol. Cell. Biol.* **14**, 1075-1083. doi:10.1128/mcb.14.2.1075-1083.1994

Mitchison, J. M. and Nurse, P. (1985). Growth in cell length in the fission yeast *Schizosaccharomyces pombe*. *J. Cell Sci.* **75**, 357-376. doi:10.1242/jcs.75.1.357

Motegi, F., Arai, R. and Mabuchi, I. (2001). Identification of two type V myosins in fission yeast, one of which functions in polarized cell growth and moves rapidly in the cell. *Mol. Biol. Cell* **12**, 1367-1380. doi:10.1091/mbc.12.5.1367

Perez, P., Soto, T., Gómez-Gil, E. and Cansado, J. (2020). Functional interaction between Cdc42 and the stress MAPK signaling pathway during the regulation of fission yeast polarized growth. *Int. Microbiol.* **23**, 31-41. doi:10.1007/s10123-019-00072-6

Philips, J. and Herskowitz, I. (1998). Identification of Kel1p, a kelch domain-containing protein involved in cell fusion and morphology in *Saccharomyces cerevisiae*. *J. Cell Biol.* **143**, 375-389. doi:10.1083/jcb.143.2.375

Qu, Y., Cao, H., Huang, P., Wang, J., Liu, X., Lu, J. and Lin, F. C. (2022). A kelch domain cell end protein, PoTea1, mediates cell polarization during appressorium morphogenesis in *Pyricularia oryzae*. *Microbiol. Res.* **259**, 126999. doi:10.1016/j.micres.2022.126999

Riquelme, M., Reynaga-Peña, C. G., Gierz, G. and Bartnicki-García, S. (1998). What determines growth direction in fungal hyphae? *Fungal Genet. Biol.* **24**, 101-109. doi:10.1006/fgbi.1998.1074

Riquelme, M., Roberson, R. W., McDaniel, D. P. and Bartnicki-Garcia, S. (2002). The effects of *ropy*-1 mutation on cytoplasmic organization and intracellular motility in mature hyphae of *Neurospora crassa*. *Fungal Genet. Biol.* **37**, 171-179. doi:10.1016/S1087-1845(02)00506-6

Riquelme, M., Aguirre, J., Bartnicki-García, S., Braus, G. H., Feldbrügge, M., Fleig, U., Hansberg, W., Herrera-Estrella, A., Kämper, J., Kück, U. et al. (2018). Fungal morphogenesis: from the polarized growth of hyphae to complex reproduction and infection structures. *Microbiol. Mol. Biol. Rev.* **82**, e00068-00017. doi:10.1128/MMBR.00068-17

Rogers, A. M., Taylor, R. and Egan, M. J. (2024). The cell-end protein Tea4 spatially regulates hyphal branch initiation and appressorium remodeling in the blast fungus *Magnaporthe oryzae*. *Mol. Biol. Cell* **35**, br2. doi:10.1091/mbc.E23-06-0214

Schuster, M., Martin-Urdiroz, M., Higuchi, Y., Hacker, C., Kilaru, S., Gurr, S. J. and Steinberg, G. (2016). Co-delivery of cell-wall-forming enzymes in the same vesicle for coordinated fungal cell wall formation. *Nat. Microbiol.* **1**, 16149. doi:10.1038/nmicrobiol.2016.149

Smith, J. A. and Rose, M. D. (2016). Kel1p mediates yeast cell fusion through a Fus2p- and Cdc42p-dependent mechanism. *Genetics* **202**, 1421-1435. doi:10.1534/genetics.115.185207

Snaith, H. A. and Sawin, K. E. (2003). Fission yeast mod5p regulates polarized growth through anchoring of tea1p at cell tips. *Nature* **423**, 647-651. doi:10.1038/nature01672

Snaith, H. A., Samejima, I. and Sawin, K. E. (2005). Multistep and multimode cortical anchoring of tea1p at cell tips in fission yeast. *EMBO J.* **24**, 3690-3699. doi:10.1038/sj.emboj.7600838

Snell, V. and Nurse, P. (1994). Genetic analysis of cell morphogenesis in fission yeast - a role for casein kinase II in the establishment of polarized growth. *EMBO J.* **13**, 2066-2074.

Taheri-Talesh, N., Horio, T., Araujo-Bazan, L., Dou, X., Espeso, E. A., Penalva, M. A., Osmani, A. and Oakley, B. R. (2008). The tip growth apparatus of *Aspergillus nidulans*. *Mol. Biol. Cell* **19**, 1439-1449. doi:10.1091/mbc.e07-05-0464

Takeshita, N., Higashitsuji, Y., Konzack, S. and Fischer, R. (2008). Apical sterol-rich membranes are essential for localizing cell end markers that determine growth directionality in the filamentous fungus *Aspergillus nidulans*. *Mol. Biol. Cell* **19**, 339-351. doi:10.1091/mbc.e07-06-0523

Takeshita, N., Diallinas, G. and Fischer, R. (2012). The role of flotillin FloA and stomatin StoA in the maintenance of apical sterol-rich membrane domains and polarity in the filamentous fungus *Aspergillus nidulans*. *Mol. Microbiol.* **83**, 1136-1152. doi:10.1111/j.1365-2958.2012.07996.x

Takeshita, N., Mania, D., Herrero De Vega, S., Ishitsuka, Y., Nienhaus, G. U., Podolski, M., Howard, J. and Fischer, R. (2013). The cell-end marker TeaA and the microtubule polymerase AlpA contribute to microtubule guidance at the hyphal tip cortex of *Aspergillus nidulans* to provide polarity maintenance. *J. Cell Sci.* **126**, 5400-5411. doi:10.1242/jcs.129841

Takeshita, N., Manck, R., Grün, N., De Vega, S. and Fischer, R. (2014). Interdependence of the actin and the microtubule cytoskeleton during fungal growth. *Curr. Opin. Microbiol.* **20**, 34-41. doi:10.1016/j.mib.2014.04.005

Takeshita, N., Evangelinos, M., Zhou, L., Somera-Fajardo, R. A., Lu, L., Takaya, N., Nienhaus, G. U. and Fischer, R. and Fischer, R. and (2017). Pulses of Ca^{2+} coordinate actin assembly and exocytosis for stepwise cell extension. *Proc. Natl. Acad. Sci. USA* **114**, 5701-5706. doi:10.1073/pnas.1700204114

Tatebe, H., Shimada, K., Uzawa, S., Morigasaki, S. and Shiozaki, K. (2005). Wsh3/Tea4 is a novel cell-end factor essential for bipolar distribution of Tea1 and protects cell polarity under environmental stress in *S. pombe*. *Curr. Biol.* **15**, 1006-1015. doi:10.1016/j.cub.2005.04.061

Tatebe, H., Nakano, K., Maximo, R. and Shiozaki, K. (2008). Pom1 DYRK regulates localization of the Rga4 GAP to ensure bipolar activation of Cdc42 in fission yeast. *Curr. Biol.* **18**, 322-330. doi:10.1016/j.cub.2008.02.005

Tay, Y. D., Leda, M., Goryachev, A. B. and Sawin, K. E. (2018). Local and global Cdc42 guanine nucleotide exchange factors for fission yeast cell polarity are coordinated by microtubules and the Tea1-Tea4-Pom1 axis. *J. Cell Sci.* **131**, jcs216580. doi:10.1242/jcs.216580

Valinluck, M., Worarattanadharm, T., Lu, C. Y., Quintanilla, R. H., Jr. and Banuett, F. (2014). The cell end marker Tea4 regulates morphogenesis and

pathogenicity in the basidiomycete fungus *Ustilago maydis*. *Fungal Genet. Biol.* **66**, 54-68. doi:10.1016/j.fgb.2014.02.010

Verde, F., Mata, J. and Nurse, P. (1995). Fission yeast cell morphogenesis: identification of new genes and analysis of their role during the cell cycle. *J. Cell Biol.* **131**, 1529-1538. doi:10.1083/jcb.131.6.1529

Ward, M. and Turner, G. (1986). The ATP synthase subunit 9 gene of *Aspergillus nidulans*: sequence and transcription. *Mol. Gen. Genet.* **205**, 331-338. doi:10.1007/BF00430447

Wernet, N., Wernet, V. and Fischer, R. (2021). The small-secreted cysteine-rich protein CyrA is a virulence factor of *Duddingtonia flagrans* during the *Caenorhabditis elegans* attack. *PLoS Pathog.* **17**, e1010028. doi:10.1371/journal.ppat.1010028

Wernet, V., Kriegler, M., Kumpost, V., Mikut, R., Hilbert, L. and Fischer, R. (2023). Synchronization of oscillatory growth prepares fungal hyphae for fusion. *eLife* **12**, e83310. doi:10.7554/eLife.83310

Youssar, L., Wernet, V., Hensel, N., Yu, X., Hildebrand, H.-G., Schreckenberger, B., Kriegler, M., Hetzer, B., Frankino, P., Dillin, A. et al. (2019). Intercellular communication is required for trap formation in the nematode-trapping fungus *Duddingtonia flagrans*. *PLoS Genet.* **15**, e1008029. doi:10.1371/journal.pgen.1008029

Yu, X., Hu, X., Mirza, M., Wernet, N., Kirschhöfer, F., Brenner-Weiß, G., Keller, J., Bunzel, M. and Fischer, R. (2021). Fatal attraction of *Caenorhabditis elegans* to predatory fungi through 6-methyl-salicylic acid. *Nat. Commun.* **12**, 5462. doi:10.1038/s41467-021-25535-1

Table S1. *A. flagrans* strains used in this study.

Strain	Description	Reference
WT	CBS 349.94	CBS-KNAW
sVW44	*teaA(p)::teaA::GFP; trpC(p)::hph::trpC(t)*	This study
sMK50	*teaC(p)::teaC::GFP; trpC(p)::hph::trpC(t)*	This study
sMK51	*teaR(p)::GFP::teaR; trpC(p)::hph::trpC(t)*	This study
sMK52	*teaA::hph (ΔteaA); trpC(p)::hph::trpC(t)*	This study
sJW01	*teaC::hph (ΔteaC); trpC(p)::hph::trpC(t)*	This study
sMK53	*teaR::hph (ΔteaR); trpC(p)::hph::trpC(t)*	This study
sMK54	*ΔteaA; trpC(p)::hph::trpC(t); nipA(p)::nipA::mCherry; gpdA(p)::neo::trpC(t)*	This study
sMK55	*ΔteaC; trpC(p)::hph::trpC(t) nipA(p)::nipA::mCherry; gpdA(p)::neo::trpC(t)*	This study
sMK56	*ΔteaR; trpC(p)::hph::trpC(t); nipA(p)::nipA::mCherry; gpdA(p)::neo::trpC(t)*	This study
sMK57	*ΔteaA; trpC(p)::hph::trpC(t); teaA(p)::teaA::teaA(t); gpdA(p)::neo::trpC(t)*	This study
sMK58	*ΔteaC; trpC(p)::hph::trpC(t); teaC(p)::teaC::teaC(t); gpdA(p)::neo::trpC(t)*	This study
sMK59	*ΔteaR; trpC(p)::hph::trpC(t); teaR(p)::teaR::teaR(t); gpdA(p)::neo::trpC(t)*	This study
sMK60	*ΔteaR; trpC(p)::hph::trpC(t); teaA(p)::teaA::GFP; gpdA(p)::neo::trpC(t)*	This study
sMK61	*teaA(p)::teaA::GFP; trpC(p)::hph::trpC(t); tubA(p)::mCherry::chsB::chsB(t); gpdA(p)::neo::trpC(t)*	This study
sMK62	*oliC(p)::teaA; trpC(p)::hph::trpC(t)*	This study

Table S2. Plasmids used in this study.

Name	Description	Reference
pVW118	*tubA(p)::mCherry::chsB::chsB(t); gpdA(p)::neo::trpC(t)*	Valentin Wernet (Karlsruhe)
pVW150	*teaA(p)::teaA::GFP; trpC(p)::hph::trpC(t)*	Valentin Wernet (Karlsruhe)
pNH58	Plasmid contraining *GFP::hph*	Nicole Wernet (Karlsruhe)
pJM16	*nipA(p)::nipA::mCherry; gpdA(p)::neo::trpC(t)*	Jennifer Emser (Karlsruhe)
pMK50	*teaC(p)::teaC::GFP; trpC(p)::hph::trpC(t)*	This study
pMK51	*teaR(p)::GFP::teaR; trpC(p)::hph::trpC(t)*	This study
pMK52	*teaA::hph (ΔteaA); trpC(p)::hph::trpC(t)*	This study
pMK53	*teaC::hph (ΔteaC); trpC(p)::hph::trpC(t)*	This study
pMK54	*teaR::hph (ΔteaR); trpC(p)::hph::trpC(t)*	This study
pMK58	*teaA(p)::teaA::teaA(t); gpdA(p)::neo::trpC(t)*	This study
pMK59	*teaC(p)::teaC::teaC(t); gpdA(p)::neo::trpC(t)*	This study
pMK60	*teaR(p)::teaR::teaR(t); gpdA(p)::neo::trpC(t)*	This study
pMK61	*teaA(p)::teaA::GFP; gpdA(p)::neo::trpC(t)*	This study
pMK62	*oliC(p)::teaA; trpC(p)::hph::trpC(t)*	This study

Table S3. Oligonucleotides used in this study.

Name	Sequence (5´ to 3´)	Description
N-ter-Pro.teaR-fw1	GATGGCTCGAGTTTTTCAGCAAGAT CATCTGCTGCATTGACTGCA	*teaR-GFP*
N-ter-Pro.teaR-rev2	TACTTACCTCACCCTTGGAAACCATGGTGAA GGGTTTCCGGATTC	*teaR-GFP*
N-ter-GFP.teaR-fw3	CGAGCGAATCCGGAAACCCTTCACC ATG GTT TCC AAG GGT GAG GTA	*tear-GFP*
N-ter-GFP.teaR-rev4	CTCGAGATGCAGTGATGCTTGCCATAGCGGC CGCTTTGTAAAGTT	*teaR-GFP*
N-ter-ORF.teaR-fw5	GGATGAACTTTACAAAGCGGCCGCT ATG GCA AGC ATC ACT GCA TC	*tear-GFP*
N-ter-ORF.teaR-rev6	GTTGACCTCCACTAGCATTACACTTATCTGGC TCTCGTCGCGG	*tear-GFP*
teaA-LB-iL-fw	GATGGCTCGAGTTTTTCAGCAAGAT ACT CGA ATC CCA ACT AGA AGC	*teaA-GFP*
teaA-LB-iL-rev	GATTACTTACCTCACCCTTGGAAAC GAACATGCCGTTGGAGTTCA	*teaA-GFP*
teaA-GFP-iL-fw	AACCATGAACTCCAACGGCATGTTC GTT TCC AAG GGT GAG GTA AG	*teaA-GFP*
teaA-GFP-iL-rev	AACGCAATGCAATGTAATAGATACC ctaAGCGGCCGCTTTGTAAA	*teaA-GFP*
teaA-RB-iL-fw	ATGCTCTTTCCCTAAACTCCCCCCA ACG ATC ACG ATT AAA GCG AAA AC	*teaA-GFP*
teaA-RB-iL-rev	ATTGTAGGAGATCTTCTAGAAAGATTGATCCT AAAATCAAGTCAATTGAT	*teaA-GFP*
teaC-LB-iL-fw	GATGGCTCGAGTTTTTCAGCAAGATCGGATC GGCTTTTGAAGAGG	*teaC-GFP*
teaC-LB-iL-rev	GATTACTTACCTCACCCTTGGAAACCCGTCG CGACTTCATGTACC	*teaC-GFP*
teaC-GFP-iL-fw	TGAACGGTACATGAAGTCGCGACGGGTTTCC AAGGGTGAGGTAAG	*teaC-GFP*
teaC-GFP-il-rev	GTTGACCTCCACTAGCATTACACTTCTAAGC GGCCGCTTTGTAAA	*teaC-GFP*
teaC-RB-iL-fw	ATGCTCTTTCCCTAAACTCCCCCCAACACGC CGCCCTCCTAAACT	*teaC-GFP*
teaC-RB-iL-rev	ATTGTAGGAGATCTTCTAGAAAGATCAGGTA CCAACCTCGTTATA	*teaC-GFP*

Fw-teaR-LB	GATGGCTCGAGTTTTTCAGCAAGAT TGA CTT CGT CTC CAT CTC ATC	Deletion *teaR*
Rev-TeaR-LB	GTTGACCTCCACTAGCATTACACTT GGTGAAGGGTTTCCGGATTC	Deletion *teaR*
Fw-teaR-RB	ATGCTCTTTCCCTAAACTCCCCCCA TCT TTT ATT CTG CAA AGC AAC AAC	Deletion *teaR*
Rev-teaR-RB	ATTGTAGGAGATCTTCTAGAAAGAT TGTAGGTATGGGGTAGAACG	Deletion *teaR*
teaA-LB-fw	GATGGCTCGAGTTTTTCAGCAAGATCTGTATT GGATTGTATTGTA	Deletion *teaA*
teaA-LB-rev	GTTGACCTCCACTAGCATTACACTTGGTGAA AGATCAGGACAGGA	Deletion *teaA*
teaA-RB-fw	ATGCTCTTTCCCTAAACTCCCCCCAACGATCA CGATTAAAGCGAA	Deletion *teaA*
teaA-RB-rev	ATTGTAGGAGATCTTCTAGAAAGATAAGGCC CTAAATAGGACATT	Deletion *teaA*
teaC-LB-fw	GATGGCTCGAGTTTTTCAGCAAGATTTCAAC CTCTTGTTTCAGCT	Deletion *teaC*
teaC-LB-rev	GTTGACCTCCACTAGCATTACACTTGCCTCTT GACTAAGAGTATT	Deletion *teaC*
teaC-RB-fw	ATGCTCTTTCCCTAAACTCCCCCCAACACGC CGCCCTCCTAAACT	Deletion *teaC*
teaC-RB-rev	ATTGTAGGAGATCTTCTAGAAAGATTTCAGGT ACCAACCTCGTTA	Deletion *teaC*
teaA-OE-fw	CTCCATCACATCACAATCGATCCAAATGGCC TTCTTATTCAAAAA	Overexpression *teaA*
teaA-OE-rev	TAATCATACATCTTATCTACATACGTTAGAAC ATGCCGTTGGAGT	Overexpression teaA
teaA-re-fw	ATGCTCTTTCCCTAAACTCCCCCCACTGTATT GGATTGTATTGTA	*ΔteaA* complementation
teaA-re-rev	ACTTTTGAGCAGCCAAATTCTCACATTAGAAC ATGCCGTTGGAGT	*ΔteaA* complementation
teaC-re-fw	ATGCTCTTTCCCTAAACTCCCCCCATTCAACC TCTTGTTTCAGCT	*ΔteaA* complementation
teaC-re-rev	ACTTTTGAGCAGCCAAATTCTCACACTACCGT CGCGACTTCATGT	*ΔteaC* complementation
teaR-re-fw	ATGCTCTTTCCCTAAACTCCCCCCATGACTTC GTCTCCATCTCAT	*ΔteaR* complementation

teaR-re-rev	ACTTTTGAGCAGCCAAATTCTCACACTACATG ATTGTACAACCGC	*ΔteaR* complementation
teaA-GFP-neo-fw	TCATACCCCGCGACGAGAGCCAGATGGTATC TATTACATTGCATTGCG	*teaA-GFP in ΔteaR*
teaA-GFP-neo-rev	ATTGTAGGAGATCTTCTAGAAAGATTGGG GGAGTTTAGGGAAA	*TeaA-GFP in ΔteaR*
qPCR-teaA-fw	GAGGTTAGCACAAGCTATGC	qPCR *teaA*
qPCR-teaA-rev	CGAGTTGACGGTGTCGAC	qPCR *teaA*

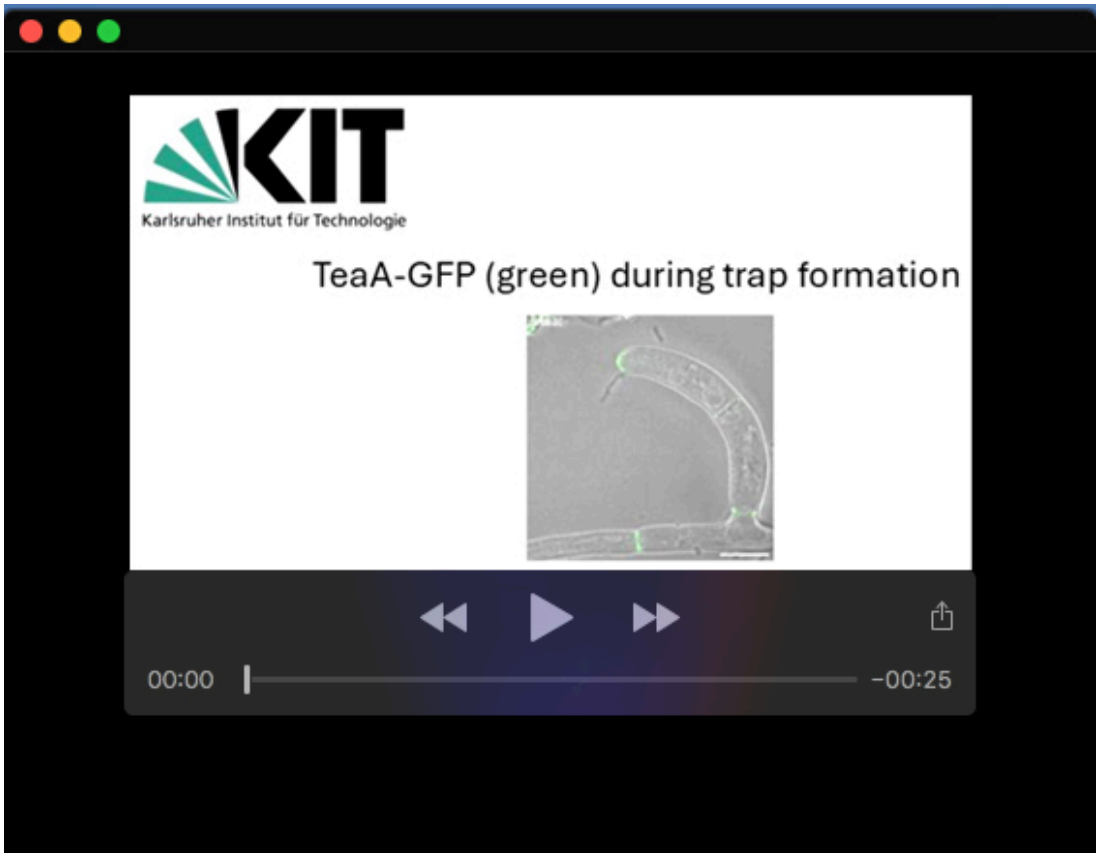

Movie 1. TeaA-GFP localization during trap formation.

Movie 2. TeaA-GFP in green and the cell membrane staining FM4-64 in red during hyphal growth.

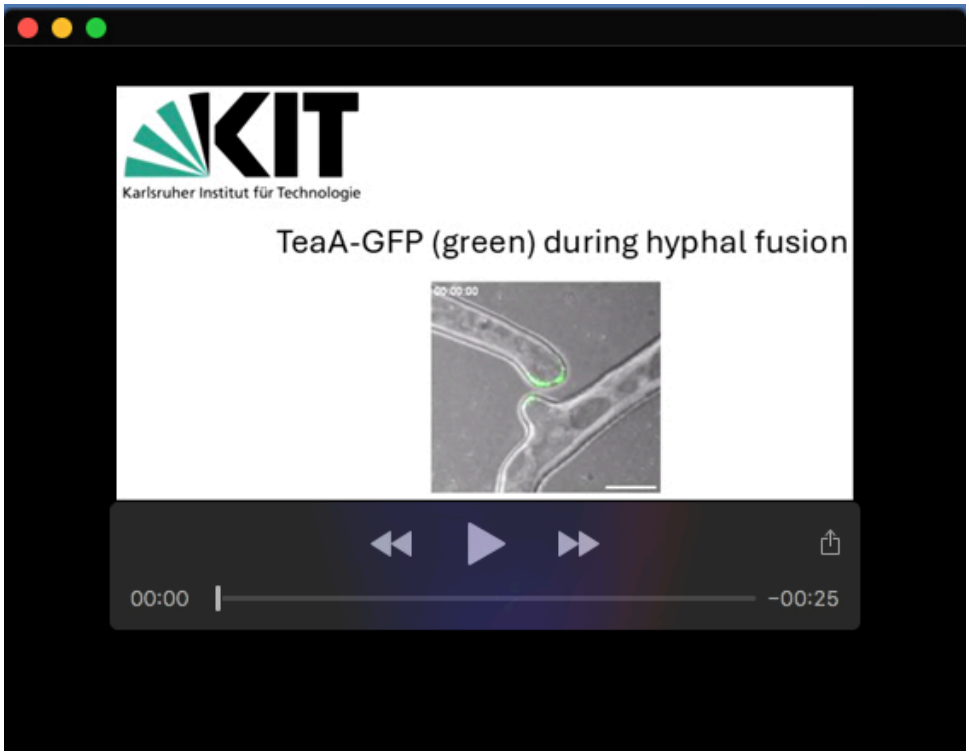

Movie 3. TeaA-GFP during hyphal fusion.